SHORT REPORTS

0955-2219(95)00212-X

Journal of the European Ceramic Society 16 (1996) 907–910

0955-2219/96/$15.00 +.00

Effect of Cu-Implanted Joining Interface on Oxygen Grain Boundary Diffusion in $SrTiO_3$ Bicrystal

I. Sakaguchi, A. Watanabe & H. Haneda

National Institute for Research in Inorganic Materials, Namiki 1-1 Tsukuba, Ibaraki 305, Japan

(Received 13 March 1995; revised version received 13 November 1995; accepted 29 November 1995)

Abstract

The oxygen tracer diffusion coefficient has been measured across the interface in a $SrTiO_3$ bicrystal by secondary ion mass spectrometry (SIMS). One part of the faces of the bicrystal were carried out on Cu implantation prior to joining. The determined volume and grain boundary diffusion coefficients are $1{\cdot}4 \times 10^{-18}$ m^2/s and $4{\cdot}5 \times 10^{-21}$ m^3/s, respectively. The enhancement of oxygen grain boundary diffusion is found. Dislocation networks and precipitates at the interface are observed using a transmission electron microscope (TEM). This observation suggests that the predominant diffusion path is along the dislocation networks. The enhancement of the oxygen diffusion in the grain boundary is due to the effect of the Cu-implanted layer.

1 Introduction

Strontium titanate ($SrTiO_3$) is widely known as an oxygen sensor at high temperature. The response time depends on oxygen bulk diffusion and the surface exchange processes. Therefore the oxygen diffusion in $SrTiO_3$ is being studied intensively these days. The dependence of the oxygen diffusivity on the oxygen vacancy concentration has been measured in polycrystalline $SrTiO_3$ with the various dopants[1,2] and in the single crystal as well.[3–5] High diffusivity paths for the oxygen in single-crystal $SrTiO_3$ have been shown to play an important role in the redox reaction.[6] Oxygen grain boundary diffusion in (110)–(110) and (100)–(100) bicrystal $SrTiO_3$, joined by hot isostatic pressing (HIP), has been investigated using secondary ion mass spectrometry (SIMS).[7] The data show that the oxygen grain boundary diffusion along the (110) joined sample is one order of magnitude larger than that in the (100) joined sample. This difference in oxygen grain boundary diffusion is explained by the difference in the grain boundary orientation.

The effect of ion implantation on strontium titanate has been extensively investigated. It has been shown that crystallization kinetics of $SrTiO_3$ is affected by the presence of water vapor.[8,9] Simpson *et al.*[10] have shown that water vapor reduces the activation energy of crystallization from 2·1 to 1·0 eV. Moreover, a study involving the implantation of 2 MeV Ar or F ions, suggested that the oxygen vacancies remained in the implanted layer after complete recovery of radiation damage by the thermal annealing.[11]

The objective of this study is to investigate the effect of the implanted layer on the oxygen grain boundary diffusion at the joining interface in a $SrTiO_3$ bicrystal with secondary ion mass spectrometry (SIMS) and transmission electron microscopy (TEM).

2 Experimental

Single-crystal $SrTiO_3$ plates with (110) polished surface and doped with Nb in 1000 ppm (Earth Jewelry Co.) were used in this study. The Cu ions were implanted at an energy of 462 keV with a dose of $1{\cdot}4 \times 10^{15}$ ions/cm^2. The implanted samples were joined in the same crystallographic planes by hot isostatic pressing (HIP). The HIP was completed in 2 h at a temperature of 1573 K and a pressure of 130 MPa.[12] The preparation of $SrTiO_3$ bicrystals has been described by Watanabe *et al.*[12] The joined bicrystal was cut perpendicular to the joining interface with a low speed diamond saw and was polished using a sequence of various grades of diamond pastes to obtain a mirror finish.

Immediately after polishing and cleaning, the sample was loaded into the exchange apparatus. The system was then closed and evacuated, and enriched $^{18}O_2$ was introduced into the manifold at 130 torr pressure. The temperature was increased to 1325 K and maintained at that value for 1800 s. After isotopic exchange of the ^{18}O between the gaseous phase and the samples, the furnace was

switched off. The $^{18}O_2$ was recovered by opening the manifold to an absorption pump which was cooled with liquid nitrogen.

Oxygen isotope profiles were obtained by a CAMECA IMS-4f instrument equipped with a cesium ion source, using a 10 kV, 5 nA, Cs^+ primary ions. The rastered area was 100 × 100 μm. The Cameca normal-induced electron gun was used to stabilize the charge build-up at the sample surface. $^{18}O^-$ and $^{16}O_2^-$ signals from the crater were acquired using a resistive anode encoder (RAE). The ratio of $^{16}O^-/^{16}O_2^-$ was measured using an electron multiplier (EM). The measured bicrystal sample is illustrated in Fig. 1. The spatial resolution of the RAE in this measurement was 3 μm. This value is much larger than the thickness of grain boundary and the Cu-implanted layer. The oxygen profile was collected from the area of 20 × 20 μm including the joining interface in $^{18}O^-$ and $^{16}O_2^-$ images measured by RAE. The oxygen isotope concentration was evaluated as follows; $C = I(^{18}O) / [I(^{16}O) + I(^{18}O)]$, where $I(^{16}O)$ and $I(^{18}O)$ are the intensities of $^{16}O^-$ and $^{18}O^-$ signals, respectively. Depth calibration was performed with a Dektak 3030 surface profiler.

Transmission electron microscopy (TEM) was used to characterize the morphology in the joined interface in bicrystal sample. The sample for TEM observation was first mechanically polished to 30 μm and then ion-milled at room temperature with 4 kV argon ions. TEM images were obtained using a JEOL 2000 EX transmission electron microscope operating at 200 kV.

3 Results and Discussion

The oxygen diffusion profile in the sample annealed at 1325 K for 1800 s is shown in Fig. 2. The oxygen diffusion profile comprised of two parts: volume diffusion up to a depth of 200 nm from the surface and the grain boundary diffusion from a depth of 700 nm. The volume diffusion contribution in the profile was fitted to a solution of diffusion equation for a constant concentration at surface as follows:[13]

$$\frac{C - C_{bg}}{C_s - C_{bg}} = erfc\left(\frac{x}{\sqrt{4D_v t}}\right) \quad (1)$$

where C is the ^{18}O concentration at depth x, C_{bg} the background natural abundance of ^{18}O, and C_s the surface concentration of ^{18}O. This equation assumes equilibrium between the gas phase and the crystal surface and hence a constant C_s value. D_v and t are the volume diffusion coefficient and

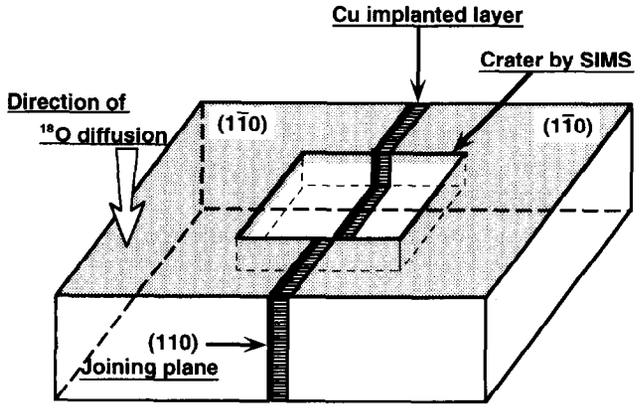

Fig. 1. Schematic diagram of a bicrystal sample.

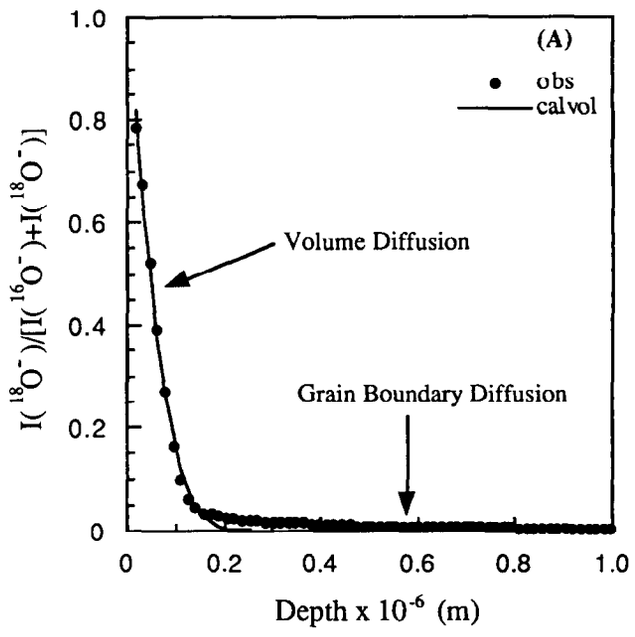

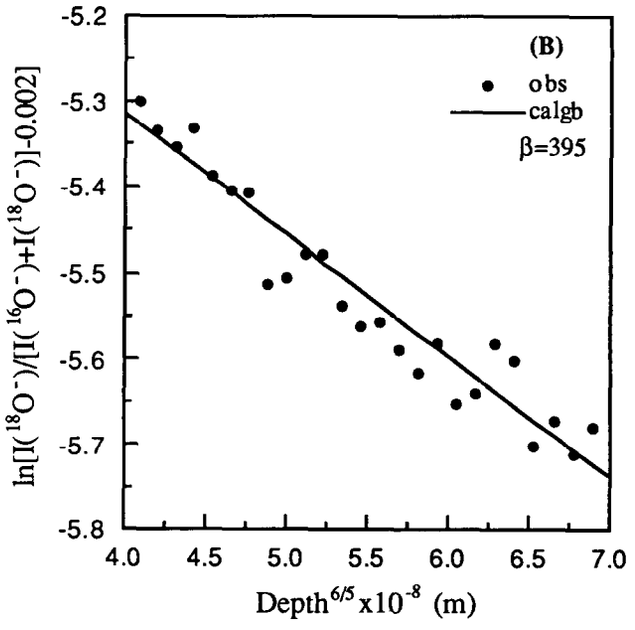

Fig. 2. Oxygen diffusion profiles obtained by SIMS. The solid squares show the oxygen isotope fraction corrected by SIMS. The solid lines indicate the theoretical curves for volume and grain boundary diffusion, respectively. The β factor is obtained from the analysis of reference.[14]

annealing time. The grain boundary diffusion coefficients were determined from the grain boundary model of LeClaire.[14]

$$\delta D_{gb} = 0{\cdot}66\left(-\frac{d\ln C}{dx^{6/5}}\right)^{-5/3}\left(\frac{4D_v}{t}\right)^{1/2} \quad (2)$$

where δ and D_{gb} are grain boundary width and grain boundary diffusion coefficient. The fitted curves shown in Fig. 2 are calculated from the above equations. The values of D_v and δD_{gb} thus obtained are $1{\cdot}4 \times 10^{-18}$ m^2/s and $4{\cdot}5 \times 10^{-21}$ m^3/s, and are shown in Fig. 3. The oxygen grain boundary diffusion along the joining interface in $SrTiO_3$ bicrystal has been reported in our previous study.[7] The value of D_v in this study is in good agreement with the previous result. However, the D_v on oxygen in 1000 ppm Nb-doped $SrTiO_3$ is 4 orders of magnitude smaller than those in pure material.[3] Chan *et al.*[15] have reported the defect chemistry of polycrystalline $SrTiO_3$. At 1000 ppm Nb-doped $SrTiO_3$, the replacement by Nb_2O_5 can be written;

$$Nb_2O_5 + V_{\ddot{O}}(-2TiO_2) \rightarrow 2Nb_{Ti}^{\cdot} + 5O_O \quad (3)$$

This suggests that the oxygen vacancy concentration decreases with the increase in the amount of Nb_2O_5 content. We believe that the difference on D_v between the pure and 1000 ppm Nb-doped $SrTiO_3$ can be explained by the above equation.

As shown in Fig. 3, the value of δD_{gb} is one order of magnitude larger than the previous result. In order to find out the characteristics of the joining interface in the bicrystal sample, a transmission electron microscope analysis (TEM) was carried out. The cross-sectional TEM micrograph near the joining interface in the bicrystal sample is shown in Fig. 4. In this micrograph, dislocations and small precipitates with diameters ranging from 20 to 60 nm are located in the band at a depth of 700 nm below the joining interface. The region from the joining interface to the band has a homogeneous texture. This TEM micrograph indicates that the damaged region of Cu-implantation clearly recovers during the HIP. The dislocation networks at the joining interface were also observed. These dislocation networks were deformed by reacting with the other dislocations. Large cubic precipitates of size 200 nm were observed to be situated mostly at the torsion point of the dislocation networks. The precipitates at the dislocation networks were formed due to the mass transport by the dislocation pipe diffusion. In the implanted sample, small precipitates were located between the large cubic precipitate on the dislocation networks and the defect band. In the non-implanted sample, the large cubic precipitate on the dislocation networks was surrounded by numerous smaller precipitates. There was no precipitate on both sides near the dislocation networks. These precipitates in non-implanted samples seem to suggest that the mass transport between the implanted and non-implanted samples is carried out through the large cubic precipitate on dislocation networks. The formation of dislocation networks at the joining interface relates to the following factors: the misalignment of two samples or the recovery of a Cu-implanted layer. The misalignment of samples occurs due to the rotation of samples for the HIP process. According to previous study,[12] the angle of misalignment in several HIP experiments is about 2°. The effects of

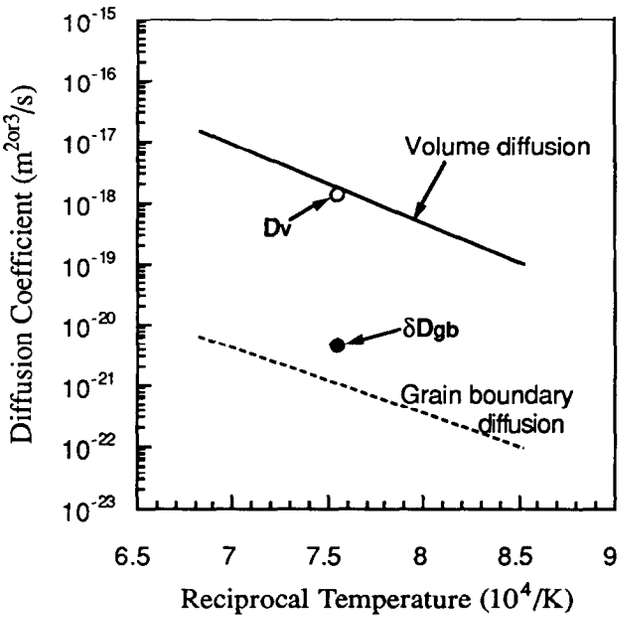

Fig. 3. Temperature dependence of oxygen diffusion coefficient for Nb-doped $SrTiO_3$. The solid and dashed lines show the temperature dependence of volume and grain boundary diffusion of oxygen in our previous result.[7]

Fig. 4. Cross-sectional TEM image in bright field at the joining interface. The upper and lower sides of the joining interface indicate the Cu-implanted and non-implanted samples. The symbols: JI, LP, and SP are the joining interface, large precipitate on the dislocation networks, and small precipitates, respectively.

Cu-implantation are considered to be that the surface region is turned into the amorphous or large amount of dislocation are introduced. The surface state after Cu-implantation has not been investigated. However, the HIP process causes the amorphous region to crystallize epitaxially with the underlying substrate when the surface is turned into the amorphous. The orientation of crystallization is same as that of the substrate. When the surface contains a large amount of dislocations, the HIP process occurs, due to the annihilation of dislocations because the interface acts as the sink for defects. In this case, the orientation of the implanted layer is also same as that of the substrate. It is considered that the formation of dislocation networks at the joining interface is due to the misalignment of the samples.

From the above discussion on the dislocation networks, it is clear that the mechanism of oxygen diffusion at the joining interface is the same as that of the non-implanted $SrTiO_3$ bicrystals (dislocation pipe diffusion).[7] The extent of dislocation pipe diffusion for other diffusion mechanisms are dependent on its density.[16] The dislocation density depends on the tilt angle and is deduced to be of the same order in several HIP experiments. Therefore, the value of the grain boundary diffusion of oxygen in this result is due to the effect of the Cu-implanted layer.

4 Conclusions

The oxygen tracer diffusion across the interface in the $SrTiO_3$ bicrystal has been measured by SIMS and TEM analysis. The determined volume and grain boundary diffusion coefficients are $1{\cdot}4 \times 10^{-18}$ m^2/s and $4{\cdot}5 \times 10^{-21}$ m^3/s, respectively. The enhancement in the oxygen grain boundary diffusion is one order of magnitude. The dislocation networks and precipitates at the joining interface have been observed. The enhancement of the oxygen grain boundary diffusion is due to the effect of the Cu-implanted layer.

Acknowledgments

The authors would like to thank Dr M. Fujimoto of Taiyo Yuden Co. Ltd for useful discussions and Mr Y. Kitami and Mr K. Kurashima of NIRIM for their support during the TEM observations.

References

1. Yamaji, A., Oxygen-ion diffusion in single-crystal and polycrystalline $SrTiO_3$. *J. Am. Ceram. Soc.*, **58** (1975) 152–3.
2. Amante, J. C. & Cawley, J. D., Oxygen tracer diffusion in $SrTiO_3$ and thin films of $YBa_2Cu_3O_{7-x}$ on $SrTiO_3$. In *Point Defects and Related Properties of Ceramics; Ceramic Transactions*, vol. 24, ed. T. O. Mason & J. L. Routbort. The American Ceramic Society, Columbus, OH, 1991, pp. 303–12.
3. Paladino, A. E., Rubin, L. G. & Waugh, J. S., Oxygen ion diffusion in single crystal $SrTiO_3$. *J. Phys. Chem. Solids*, **26** (1965) 391–7.
4. Schwarz. D. B. & Anderson, H. U., Determination of oxygen chemical diffusion coefficients in single crystal $SrTiO_3$ by capacitance manometry. *J. Electrochem Soc.*, **122** (1975) 707–10.
5. Kiessling, U., Claus, J., Borchardt, G., Weber, S. & Scherrer, S., Oxygen tracer diffusion in Lanthanum-doped single-crystal strontium titanate. *J. Am. Ceram. Soc.*, **77** (1994) 2188–90.
6. Waugh, J. S., Paladino, A. E., Dibenedetto, B. & Wantman, R., Effect of dislocations on oxidation and reduction of single-crystal $SrTiO_3$. *J. Am. Ceram. Soc.*, **46** (1963) 60.
7. Sakaguchi, I., Watanabe, A., Hishita, S. & Haneda, H., Oxygen tracer diffusion along joining interface and mechanical damage in bicrystal $SrTiO_3$. *J. Appl. Phys.* (in review).
8. White, C. W., Boatner, L. A., Sklad, P. S., McHargue, C. J., Rankin, J., Farlow, G. C. & Aziz, M. J., Ion implantation and annealing of crystalline oxides and ceramic materials. *Nucl. Instr. and Meth.*, **B32** (1988) 11–22.
9. McCallum, J. C., Rankin, J., White, C. W. & Boatner, L. A., Time resolved reflectivity measurements in Pb-implanted $SrTiO_3$. *Nucl. Instr. and Meth.*, **B46** (1990) 98–101.
10. Simpson, T. W., Mitchell, I. V., McCallum, J. C. & Boatner, L. A., Hydrogen catalyzed crystallization of strontium titanate. *J. Appl. Phys.*, **76** (1994) 2711–18.
11. Sakaguchi, I., Haneda, H., Hishita, S., Watanabe, A. & Tanaka, J., Oxygen diffusion in ion-implanted layer of Nb-doped $SrTiO_3$. *Nucl. Instr. and Meth.*, **B94** (1994) 411–16.
12. Watanabe, A., Haneda, H., Ikegami, T., Tanaka, J. & Shirasaki, S., Solid state bonding of $SrTiO_3$ single crystals using HIP. In *Proceedings of 2nd Japan International SAMPE Symposium*, Japan, 1991, pp. 11–14.
13. Crank, J., *The Mathematics of Diffusion*, Ch. 3.3. Oxford University Press, London, UK, 1975, pp. 28–43.
14. LeClaire, A. D., The analysis of grain boundary diffusion measurements. *Br. J. Appl. Phys.*, **14** (1963) 351–6.
15. Chan, N. H., Sharma, R. K. & Smyth, D. M., Nonstoichiometry in $SrTiO_3$. *J. Electrochem. Soc.*, **128** (1981) 1762–8.
16. Sakaguchi, I., Yurimoto, H. & Sueno, S., Self-diffusion along dislocations in single-crystal MgO. *Solid State Commun.*, **84** (1992) 889–93.